MSX Design Parameters Driven by Targets and Backgrounds

A. T. Stair, Jr.

The underlying requirements for demonstrating space-based surveillance, acquisition, tracking, and discrimination of ballistic reentry vehicles and penetration aids were followed in the design of the Midcourse Space Experiment (MSX) satellite and sensors. The primary sensor is the totally cryogenic Spatial Infrared Imaging Telescope III (SPIRIT III), supported by multiple co-aligned visible and ultraviolet sensors. SPIRIT III is cooled with solid hydrogen and has an expected minimal on-orbit life of 15 months. The 35-cm aperture and multiple focal planes with different spectral passbands were designed for long-range target capability and background measurements of the structure in the Earth-limb radiance. To detect and track reentry vehicles at ranges of 6000 km or more while viewing near Earth, a sensor must have an excellent off-axis reimaging optical system with a Lyot stop and superpolished primary and secondary mirrors. Superpolished cryogenic mirrors are extremely sensitive to contamination, so MSX also carries a unique suite of contamination monitoring sensors, particularly for on-orbit H_2O and particles. MSX will be the first space experiment to correlate optical contamination (changes in nonrejected Earth radiance) with the satellite environment.

INTRODUCTION

The Midcourse Space Experiment (MSX) is the Department of Defense's most unique and complete electro-optical space observatory. Its primary mission, midcourse phenomenology, and other measurement objectives and capabilities are discussed in the article by Mill and Guilmain in this issue and a previous publication.[1] Each of the multiple sensors, which in total operate from the very-long-wavelength infrared (28 μm) to the far-ultraviolet (110 nm), was designed and built specifically for the MSX mission. All of the radiometric sensors are co-aligned and hard-mounted to an optical "bench" on the spacecraft.

MSX was created primarily for infrared data collection and as a functional demonstration of the Spatial Infrared Imaging Telescope III (SPIRIT III) cryogenic sensor. It evolved from the national Midcourse Sensor

Study (MSS) sponsored by the Strategic Defense Initiative Organization (SDIO, now the Ballistic Missile Defense Organization) and the Air Force, and was hosted by MIT Lincoln Laboratory during 1987 and 1988. A major finding of that study was that space surveillance, tracking, and discrimination functions did not necessarily require the large 1-m-dia. mirrors for the infrared sensors, which had been until then a nominal design parameter.

As a result of the MSS, SPIRIT III was designed with the support of a broad aerospace community (Air Force, Army, SDIO, federally funded research and development centers, and contractors) to have a 35-cm cryogenic aperture. The issue of mirror size is critical since, historically, satellite mass and therefore costs tend to scale with mirror diameter to the 2.6 power for spaceborne electro-optical sensors. This article examines some unique DoD technical issues that will be addressed by MSX and, in particular, by the SPIRIT III infrared radiometric sensor, which was built and calibrated by the Space Dynamics Laboratory of Utah State University.

AUXILIARY INSTRUMENTS

The MSX suite of state-of-the-art ultraviolet/visible imaging spectrometers was built by APL to obtain fundamental spectroscopic data in support of the underlying physics and chemistry that produce infrared atmospheric backgrounds and target signatures. The acquisition of supporting spectral data to help interpret the infrared radiometric signatures is also the primary role of the cryogenic Fourier transform interferometer spectrometer embedded in the SPIRIT III sensor.

Fortuitously, the impressive capability of these infrared/visible/ultraviolet spectral sensors permits measurement of most of the atmospheric greenhouse gases crucial to the study of global climate changes.[2,3] The co-aligned wide and narrow field-of-view visible and ultraviolet "imagers with filters" are sensors that support the interpretation of SPIRIT III's infrared, radiometric background and radiometric target measurements. The well-known sensitivity to contamination of space-based electro-optical sensors, particularly superpolished cold mirrors for high off-axis rejection, led to the design and development of the MSX suite of contamination sensors and unique contamination control procedures.[4] The Space-Based Visible camera was included in MSX to complete the overall demonstration of the value of space surveillance such as cataloging resident space objects. This sensor, built by MIT's Lincoln Laboratory, carries an onboard signal processor to suppress background clutter, detect moving targets, and generate target reports at low data rates.[5] In addition, an onboard signal data processor built by the Hughes Corporation was designed for a parallel functional demonstration of the infrared radiometric sensor, SPIRIT III.

TARGETS AND SPIRIT III DESIGN ISSUES

Very sensitive infrared sensors are required to detect and track ballistic reentry vehicles and associated objects, day or night. Such sensors must operate in wavelength regions where these hard bodies radiate energy or reflect the Earth's radiant energy. For a 300 K gray body, 85% of the energy falls between 6 and 30 μm. The detection/tracking problem for sunlit objects can be achieved by using simpler visible sensors, which will be demonstrated by the MSX visible sensor suite. Many parameters enter into optimizing the number of satellites and constellations, the size of sensor aperture, wavelength selection, etc. In particular, these issues depend on the definition of the threat (i.e., number of threat objects and penetration aids, deployment, size, shape, temperature, emissivity, etc.). For illustrative purposes only (since MSX is an experiment rather than a prototype), the 900-km orbit and 35-cm diameter of the SPIRIT III primary mirror with a 90-μrad-pixel instantaneous field of view will be used for target and background discussions.

The spectral passbands and sensitivities of the SPIRIT III radiometer are given in Table 1. These calibrated values for the noise equivalent flux densities were obtained before the most recent refurbishment of the sensor and may vary somewhat from actual flight

Table 1. SPIRIT III radiometer passbands and calibrated sensitivities.

Band	Passband nominal 50% transmission (μm)	Noise equivalent flux densities in band ($\times 10^{-18}$ W/cm^2) Integration time 2.7 ms	Integration time 14 ms	Point source[a] 2.7 ms
A	6.0–10.9	2.5	0.5	0.6
B_1	4.22–4.36[b]	21	4.5	6.6
B_2	4.24–4.45[b]	18	3.9	5.7
C	11.1–13.2	8.6	1.8	1.6
D	13.5–16.0	5.1	1.1	2.0
E	18.3–26.0	17	3.5	11

[a]SPIRIT III has been calibrated using a 2.7-ms integration time per detector plus a time delay and integrate (TDI) process using multiple detectors (the number varies by band) and a matched filter.
[b]Bands B_1 and B_2 are reported to the most significant decimal point.

values. Bands A, C, D, and E are separate filtered focal plane arrays; bands B_1 and B_2 are implemented by filtering separate halves of one focal plane array.

Bands B_1 and B_2 are centered in the optically thick ν_3 band of CO_2 for measurements looking at the hard Earth (below the horizon). All other bands, designed for viewing into space (above the horizon), accept so much radiation that their detectors saturate owing to atmospheric limb radiance, which occurs when the sensor views below tangent heights on the order of 40 to 60 km (Fig. 1).[6] The upper altitude is set by the tangent altitude, which is equivalent to a signal-to-noise ratio of 1. Bands B_1 and B_2 will not saturate and will provide measurements of terrestrial backgrounds.

Perhaps the most critical question for spaceborne infrared sensor performance concerns range. Assume a nominal ballistic reentry vehicle to be a cone of ≈1-m length and ≈0.5-m base diameter with an emissivity of 0.5 and a temperature of 300 K. Depending on the viewing angle, the projected area varies from about 0.2 to 0.8 m^2. Using 0.3 m^2 for the projected area, the total radiant signal J is 22 W/sr. For a 300 K blackbody, about 30% of the emitted energy falls into band A (≈6 to 11 μm), resulting in an ≈6.6-W/sr target for this band. Figure 2 depicts a scenario in which the MSX sensors are observing such a reentry vehicle near apogee, which is equidistant beyond an 80-km tangent point as MSX is on the other leg. At a range of 6400 km, the target flux (irradiance) at the aperture of SPIRIT III in band A is $\approx 16 \times 10^{-18}$ W/cm^2. From Table 1, using the noise equivalent flux density for a point source with TDI of 6×10^{-19} W/cm^2 in band A, the Fig. 2 scenario would yield a measurement (independent of backgrounds) with a signal-to-noise ratio of about 25.

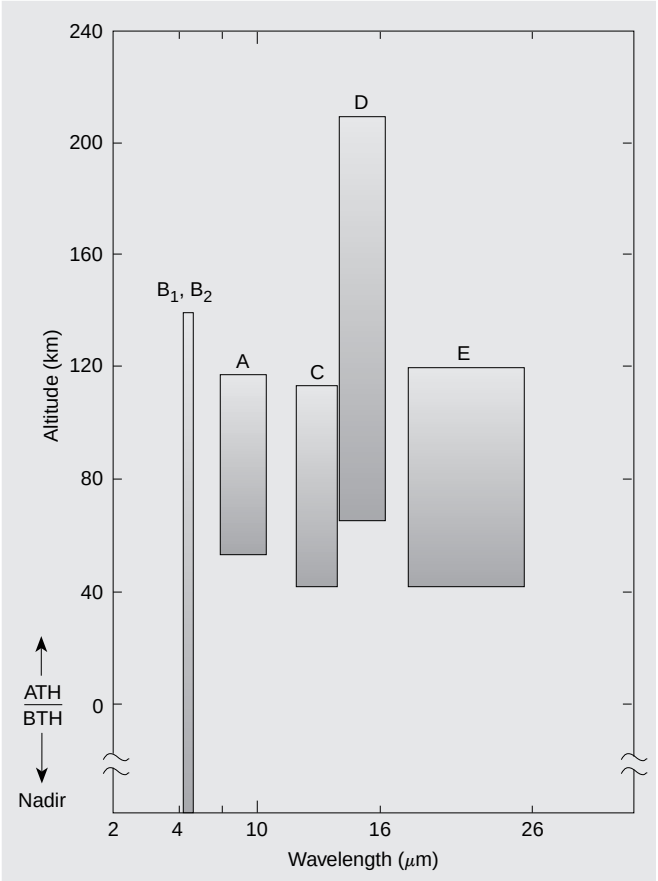

Figure 1. Radiometer bandwidths and measurement capabilities as a function of altitude (ATH and BTH = above and below the horizon, respectively). (Reprinted from Ref. 6 by permission.)

Other important target-related "global" parameters for an infrared sensor are the total field of view, the instantaneous pixel resolution, and scene revisit time. SPIRIT III has a 1° "vertical" extent, defined by the height of the column of detectors. There are 5 focal plane arrays (chips) of up to 8 columns of detectors, each with 192 detectors per column. An internal scanning mirror sweeps the vertical field of view of the radiometer over a wider field of regard and can be commanded into any one of three scan modes of 3.0, 1.5, or 0.75° nominal total angular extent. The mirror scans at a constant rate of 0.46°/s in object space, producing average revisit times of 7.17, 3.59, and 1.79 s, respectively, in the three scan modes. This variable revisit time optimizes the ability to measure the temporal variability of target signatures caused by apparent changes in temperature and projected area. The angular resolution of 90 μrad relates to the ability to observe individual objects (the classic closely spaced object problem). Since an intercontinental ballistic missile (ICBM) flies for about 30 min, one can envision objects being deployed and separating in a dimension perpendicular to the sensor–target line of sight at velocities that differ from one another by ≥1 m/s for 10 min before apogee. In such a case, at apogee, the subsequent apparent object separation of 600 m is consistent for individual object measurements in the scenario of Fig. 2, since 90 μrad × 6400 km yields a resolution of about 580 m for individual pixels of SPIRIT III.

For discrimination purposes, bands A, D, and E have overlapping fields of view and record data simultaneously by using dichroic beamsplitters and filters. Such simultaneous measurements eliminate errors due to target motion. Multiple color measurements demonstrate the capability (and limitations) of an infrared sensor to derive important target parameters such as temperature and area. In general, discrimination requires a much higher signal-to-noise ratio (i.e., SNR > 30) than do detection (SNR ≥ 6) and tracking (SNR ≥ 3). The radiation arriving at a sensor (such as SPIRIT III) due to thermal emission of a target of area a at range R is $J = \epsilon a L(T)/R^2$, where ϵ is emissivity, T is surface temperature, and L is the Planck function, which can be integrated for any particular bandpass. A two-color measurement

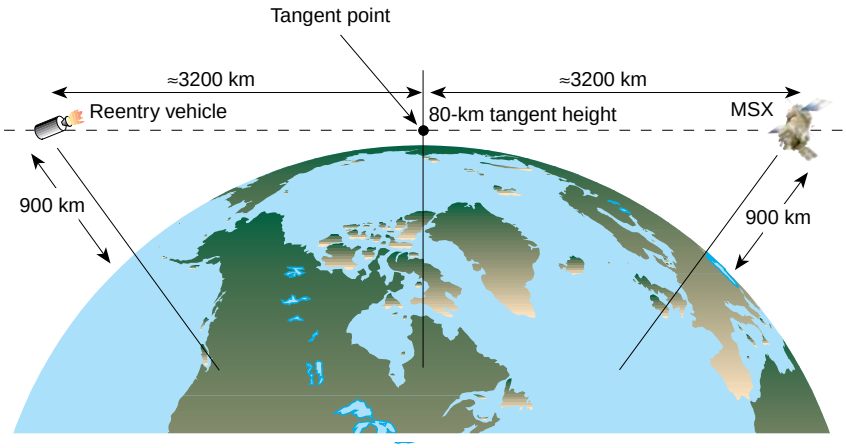

Figure 2. Geometry of MSX viewing a reentry vehicle through the Earth-limb. The target is equidistant from the tangent point at 80 km.

determines T since the ratio eliminates R, a, and ϵ when ϵ is the same in both colors. If the range R is known, then ϵa can be determined. If the emissivity is less than 1, then the derivation of area becomes much more complex, since radiation reflected by the body's surface coming from the Earth and the atmosphere must be considered. The multispectral capability of SPIRIT III (bands A, C, D, and E) will be applied to these cases. For example, the body-reflected radiation in the atmospheric "window" bands (A, C, and E) represents integrated surface "Earth shine," which can be modeled using global satellite scenes and atmospheric sounders to correct for atmospheric transmission and variable emissivities. Earth radiation in band D emanates from atmospheric CO_2 at a colder temperature since it arises from higher altitudes in the mesosphere. The complexities of such analyses must include target shape, surface composition, diffuse vs. specular reflection, emissivity/reflectivity as a function of wavelength, etc., and are the subject of specialized studies beyond the scope of this article (personal communication, H. Burke, MIT Lincoln Laboratory, 1982; also see Ref. 7).

BACKGROUNDS AND SPIRIT III DESIGN ISSUES

Atmospheric backgrounds play a significant role in the detection and tracking of reentry bodies. Figure 3 shows the atmospheric infrared spectral radiance at an 80-km tangent height.[8] Using band A (6–10.9 μm) as an example, the dominant atmospheric radiating species is O_3 and secondarily H_2O. The actual measured integrated radiance profile of ozone vs. altitude is shown in Fig. 4.[9] Ozone is optically thin (even in a limb view), and therefore radiance contributions come from higher altitudes along the line of sight; the signal, however, is dominated by radiance coming from near the tangent altitude. At the 80-km tangent height of the example in Fig. 2, the integrated nighttime radiance for band A is approximately 7×10^{-7} W/cm^2. This background presents an irradiance at the SPIRIT III aperture of about 2.8×10^{-14} W/cm^2 compared with the target irradiance of 16×10^{-18} W/cm^2 (see the previous discussion).

Since this background signal represents a nominal DC radiance that can be filtered by various forms of processors for point source detection, two questions arise: (1) How effective are the processors, and (2) what is the small-scale spatial structure of the background that, after processing, results in false signals (exceedances) above some predetermined threshold and must therefore be handled as "clutter"? If the background structure due to turbulence, gravity waves, etc., can pass through the signal processor at 0.01% of the DC level, a signal-to-clutter ratio of about 6 would result for the example discussed in Fig. 2. If the "filtered" background structure is 0.1% of the DC level, then the signal-to-clutter ratio is less than 1 and target detection and/or tracking becomes more difficult.

Referring again to Fig. 3, the integrated DC background radiance can be seen to vary among bands by more than 2 orders of magnitude: in units of

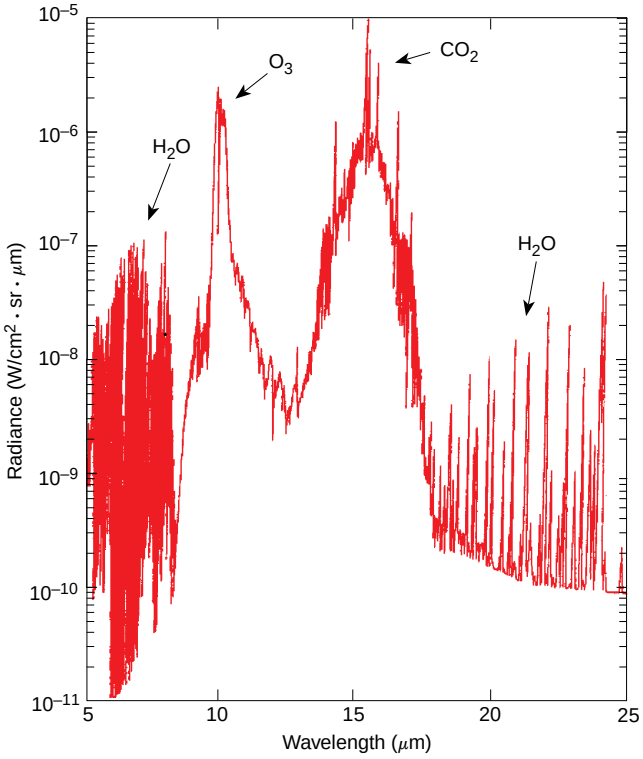

Figure 3. Predicted Earth-limb radiance at an 80-km tangent altitude, midlatitude, daytime, during the summer.

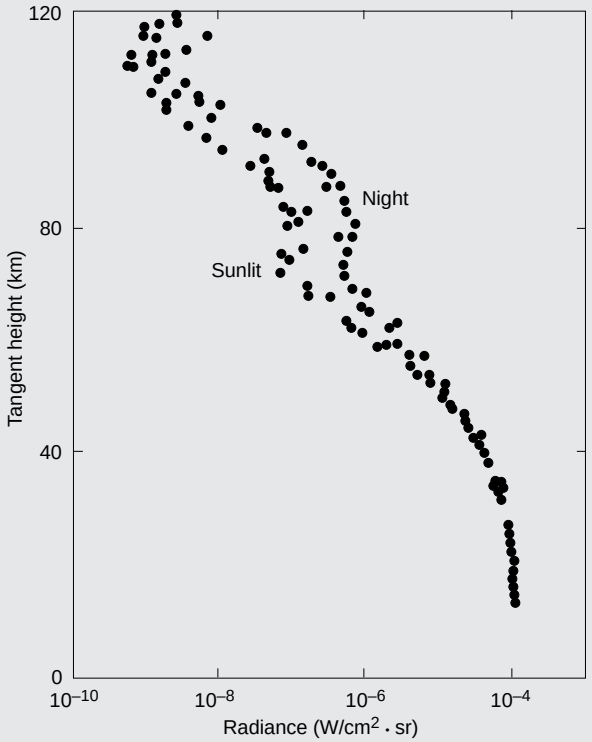

Figure 4. The measured ν_3 band radiance integrated over the wavelength region 9.2–10.5 μm as a function of tangent height. (Reprinted from Ref. 9 by permission.)

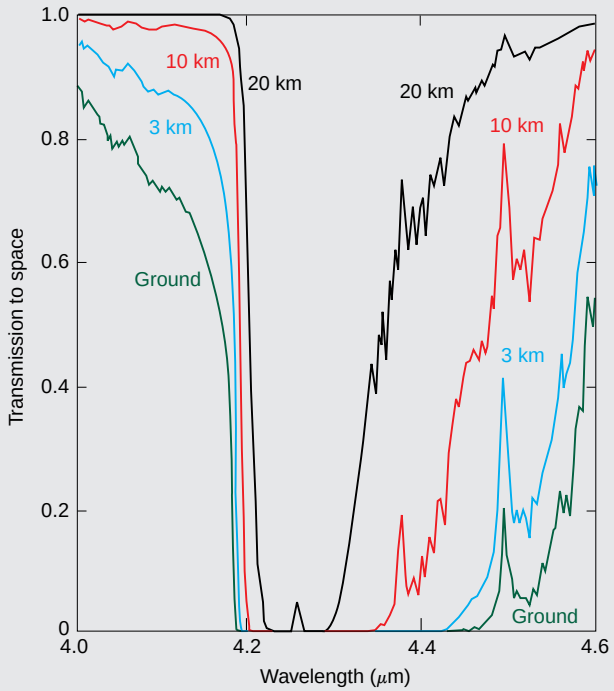

Figure 5. Atmospheric transmission, midlatitude, nadir view, during the summer.

W/cm^2·sr·μm, band A = 7.6×10^{-7}, C = 8×10^{-9}, D = 1.7×10^{-6}, and E = 1.3×10^{-9}. Therefore, sensor performance for tracking and, particularly, discrimination while viewing through the Earth-limb depends significantly on bandpass and atmospheric structure. A primary mission of MSX is to measure the background structure.

Bands B_1 and B_2, which are located in the middle wavelength infrared (MWIR) spectral region, are selected for their potential to track targets against terrestrial Earth backgrounds. For Earth viewing, the MWIR region is characterized by a very strong CO_2 absorption band, which limits the altitude as viewed from space, and therefore clutter, by careful choice of bandpass. The use of the MWIR region for tracking plumes of high-altitude ICBM stages and postboost vehicles involves the same Earth-limb and auroral background clutter issue as the other bands. In Fig. 5, the transmission to space (nadir viewing) for four altitudes (0, 3, 10, and 20 km) is plotted as a function of wavelength. Band B_1 (4.22–4.36 μm) has essentially zero transmission below 10 km; therefore, radiance from lower-altitude clouds and the ground is limited. The ground scenes and low-altitude clouds are expected to be more structured than radiance from higher altitudes. Band B_2 (4.24–4.45 μm) has some transmission down to about 3 km (≈8% at the longest wavelength) but does not see to the ground. The overall objective of bandpass selection is to optimize the target-to-clutter ratio. A nominal theater missile warm body (350 K) signal can vary by a factor of about 4 over the MWIR region as one widens the long wavelength side from 4.3 to 4.6 μm. However, the background radiance as seen from space increases by about a factor of 30 (≈3×10^{-6} to ≈1×10^{-4} W/cm^2·sr·μm), so that the clutter is expected to increase much faster than the target signal as this band is widened to the longer wavelengths. SPIRIT III's mission is to measure globally and categorize by the relevant geophysical parameters (for modeling) the spatial structure in bands B_1 and B_2.

Celestial backgrounds (for example, stars, zodiacal radiances, asteroids, etc.) are also important for surveillance sensors. Although these backgrounds were not considered design drivers, the celestial measurements obtained by MSX are significant and raise some important questions:

- How close to the Sun can an infrared sensor look to maximize coverage? (MSX sensors will measure the near-Sun zodiacal background.)
- Can the infrared stars be used for accurate goniometric purposes? (The infrared centroids will be offset from visible because of dust and gases that surround the star. The MSX sensors will measure the infrared centroids and process the data to achieve measurements on the order of a few microradians.)

- Can a surveillance sensor discriminate against the celestial background using a stored radiometric catalog and subtraction? (The Infrared Astronomy Satellite [IRAS] catalog is limited to ≈45 stars per square degree, too low for system use. SPIRIT III's resolution is about 30 times that of IRAS. MSX experimental plans are scheduled to map the galactic center to a level of 1100 stars per square degree.)

NONREJECTED EARTH RADIANCE DESIGN ISSUES

In order to detect and track the small infrared signal of a reentry vehicle as seen from space relatively near the Earth, the design of SPIRIT III had to address another major optical issue: Without the impractical use of an extremely long and cold baffle, radiation from the Earth will strike the primary mirror of the sensor telescope, and the scattered infrared light can be many orders of magnitude larger than the signal. The SPIRIT III solution to this problem was to design and fabricate an off-axis reimaging optical system with Lyot stops and baffles to reduce the amount of diffracted and scattered radiation reaching the focal plane. Ultimate performance depends on how smooth (superpolished) and clean the primary and secondary mirror surfaces are. A technical parameter used as the figure of merit is the bidirectional reflectivity distribution function (BRDF), multiplied by the functional power of the angular (θ) dependence of fall-off of the scattered radiation. The BRDF represents the angular dependence of scatter from a parallel beam per steradian.

Figure 6, which plots the nighttime atmosphere and zodiacal radiances for band C as a function of altitude, illustrates the critical role that scattered radiation plays in the measurement of backgrounds and targets. Competing radiances coming from scattered Earth shine, i.e., nonrejected Earth radiance (NRER), are shown for three different levels of contamination on superpolished mirrors.[10] The worst case of NRER shown for BRDF = $1 \times 10^{-2}\ \theta^{-1.1}$ represents an initially low scatter surface that has been treated poorly in a laboratory environment (in this case, for example, resulting from an inadvertent loss of vacuum). The example plotted for BRDF = $3 \times 10^{-3}\ \theta^{-1.5}$ is the value extrapolated for a very low scatter mirror on orbit in space after about 3 years.

Figure 7 illustrates the sensitivity of scatter (BRDF) to the thickness of H_2O collected on a superpolished mirror.[11] Outgassing of water from the multilayer insulation of SPIRIT III is modeled to produce a layer ≈1.5 μm thick in about 9 to 12 months. The best BRDF, $1 \times 10^{-4}\ \theta^{-2}$, is derived from a pristine superpolished surface such as those of the SPIRIT III primary and secondary mirrors upon installation. As illustrated in Fig. 6, the contribution of NRER for contaminated mirrors equals the atmosphere at the 70- to 80-km tangent heights. If the NRER does not vary significantly with horizontal (or vertical) angular scanning, the spatial structure of the atmosphere can still be measured, but with less accuracy. NRER from pristine mirrors does not equal the atmospheric radiance almost until the floor of the sensor noise equivalent radiance is reached. One sees, in fact, that in this band, the zodiacal backgrounds also dominate the atmospheric background above 110 km.

The radiance profiles for the other bands are spectrally dependent but will not be illustrated for the sake of brevity. The impact of contaminated optics (NRER) is worse for the sensitive long-wavelength window band E and less so for the atmospheric emission band D.

INFRARED SENSOR LIFETIME ON ORBIT

Other key and somewhat independent parameters for SPIRIT III are the amount and kind of cryogen to

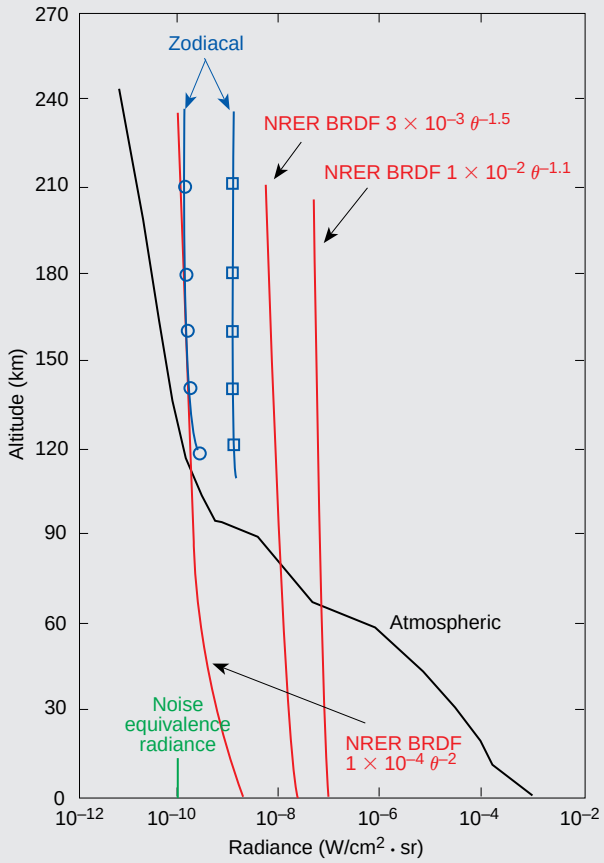

Figure 6. Components of the radiometric profile of band C in an Earth-limb viewing aspect. Atmospheric radiance, zodiacal backgrounds for two different views, and nonrejected Earth radiance (NRER) bidirectional reflectivity distribution function (BRDF) are shown (squares denote zodiacal background at elongation angle of 30° and ecliptic latitude at 0°; circles denote elongation angle of 180° and ecliptic latitude at 0°).

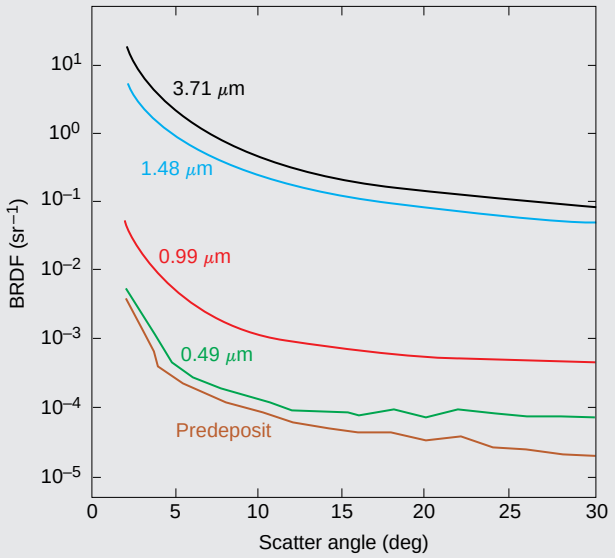

Figure 7. Bidirectional reflectivity distribution function (BRDF) degradation at selected H_2O film thicknesses (surface temperature = 27 K, wavelength = 0.6328 μm).(Reprinted from Ref. 11 by permission.)

be carried. These parameters are driven by its infrared lifetime on-orbit goal of 15 months to obtain a statistically meaningful set of background data and multiple target opportunities. A Lockheed Corporation space-qualified dewar using solid hydrogen was selected for this purpose. Other major factors affecting the experimental time on orbit are tape recorder storage, power utilization, and the telemetry downlink, which is limited to one ground station at the Applied Physics Laboratory. Much of the data will be collected and recorded at 5 MB/s and played back at 25 MB/s. The overall average data collection duty cycle is about 10% of the actual time on orbit.

SUMMARY

Despite the many changes that have occurred in concepts for ballistic missile defense over the period since MSX was designed, it is still the most complete sensor suite for demonstrating the required space functions and obtaining vital phenomenological data. Its primary role is to demonstrate the capabilities of space-based infrared wavelength technology to detect, track, and discriminate ballistic objects and collect the data needed for future system designs. Data to be obtained in the MWIR region (4.3 μm) and the medium to long-wavelength infrared region (6–11 μm) are particularly applicable to tracking theater-class missiles with large warm bodies. Data in the long-wavelength infrared region (6–16 μm), and particularly in the very-long-wavelength infrared region (16–28 μm), are critical for tracking and discriminating the smaller ICBM-class reentry vehicles and decoys. The auxiliary MSX instruments are important for understanding much of the phenomenology associated with the infrared measurements. MSX is the only sensor of its class and represents a major milestone for demonstrating ballistic missile defense technology.

REFERENCES

1. Mill, J. D., O'Neil, R. R., Price, S., Romick, G. J., Uy, O. M., Gaposchkin, E. M., and Stair, A. T., Jr., "Midcourse Space Experiment: Introduction to the Spacecraft, Instruments and Scientific Objectives," *J. Spacecr. Rockets* **31**(5), 900–907 (1994).
2. Zachor, A. S., Gallery, W. O., O'Neil, R. R., Gibson, J., Gardiner, H. A. B., Stair, A. T., Jr., and Mill, J. D., "Midcourse Space Experiment (MSX): Capabilities of the LWIR Interferometer for Remote Sensing of Trace Constituents in the Stratosphere and Mesosphere," in *Proc. SPIE International Symposium on Optical Engineering in Aerospace Sensing*, Orlando, FL, p. 2222-15 (4–8 Apr 1994).
3. Romick, G. J., Anderson, D. E., Carbary, J. F., Paxton, L. J., Meng, C. I., and Morrison, D. M., "Midcourse Space Experiment Satellite Ultraviolet and Visible Background Phenomenology," in *Proc. SPIE International Symposium on Optical Engineering in Aerospace Sensing*, Orlando, FL, p. 2223-13 (4–8 Apr 1994).
4. Uy, O. M., "Contamination Experiments in the Midcourse Space Experiment (MSX) Satellite," in *Proc. SPIE Conference on Optical System Contamination: Effects, Measurements, Control III*, Vol. 1754, International Society for Optical Engineering, pp. 170–176 (1992).
5. Gaposchkin, E. M., *Space Based Surveillance with MSX*, AAS 95-231, American Astronautical Society (Feb 1995).
6. O'Neil, R. R., Gardiner, H. A. B., Gibson, J., Humphrey, C. H., Hegblom, R., Fraser, M. E., Kendra, M., Wintersteiner, P., and Rice, C., "Midcourse Space Experiment (MSX): Plans and Capability for the Measurement of Infrared Earthlimb and Terrestrial Backgrounds," in *Proc. SPIE International Symposium on Optical Engineering in Aerospace Sensing*, Orlando, FL, p. 2223-25 (4–8 Apr 1994).
7. Allen, J. L., *The Physics of Target Discrimination in Ballistic Missile Defense Systems*, Jamieson Science and Engineering, Inc., Report sponsored by BMDO/SRE.
8. Sharma, R. D., Duff, J. W., Sunberg, R. L., Bernstein, L. S., Gruninger, J. H., Robertson, D. C., and Healey, R. J., *Description of SHARC-2, The Strategic High-Altitude Radiance Code*, PL-TR-91-2071, Air Force Philips Laboratory (also available as NTIS No. ADA 239008) (1991).
9. Stair, A. T., Jr., Sharma, R. D., Nadile, R. M., Baker, D. J., and Grieder, W. F., "Observations of Limb Radiance with Cryogenic Spectral Infrared Rocket Experiment," *J. Geophys. Res.* **90**(A10), 9763–9775 (1985).
10. Guregian, J. J., Benoit, R. J., and Wong, W. K., "Overview of Contamination Effects on the Performance of High-Stray Light-Rejection Telescope via Ground Measurements," *SPIE* **1329**, 2–15 (1990).
11. Uy, O. M., Lesho, J. C., Seiber, B. L., Bryson, R. J., and Wood, B. E., "Optical Effects of Condensates on Cryogenic Mirrors for the Midcourse Space Experiment (MSX)," in *Proc. SPIE: Cryogenic Optical Systems and Instruments VI*, Vol. 2227, pp. 54–63 (1994).

ACKNOWLEDGMENTS: The list of significant contributors is too long to recite; most are part of the MSX science teams. I wish, particularly, to acknowledge the early inputs of Barry Katz (SDIO), who is deceased and will miss the fruits of his labor. Also, the support and technical guidance of Major General Garry Schnelzer of SDIO and the Air Force, now retired, have been invaluable. The MSX mission is sponsored by the Ballistic Missile Defense Organization. This work was supported under SDIO contract 84-90-C005.

THE AUTHOR

A. T. STAIR, JR., received a B.S. degree in mathematics (1952) and a Ph.D. in physics (1956) from the University of Oklahoma. He began his career studying the physics and chemistry of the atmosphere at the Air Force Cambridge Research Laboratory in 1956, retiring in 1986 as Chief Scientist of the Air Force Geophysics Laboratory. He has authored or co-authored over 100 papers and is an adjunct professor with Utah State University. Dr. Stair has directed a number of national scientific studies for the Air Force and SDIO (BMDO). He served 4 years as a member of the Air Force's Scientific Advisory Board, was a member of Vice President Gore's Environmental Task Force, and continues as a member of the follow-on organization, Medea. He belongs to Phi Beta Kappa and Sigma Xi, and was elected to the Oklahoma Hall of Fame in 1987. Dr. Stair joined Visidyne, Inc., of Burlington, Massachusetts, as Senior Vice President in 1994. His e-mail address is ats@bur.visidyne.com.